
A Convergence-Guaranteed Algorithm for Stochastic Optimal Control Problems

Mohsen Amidzadeh

Department of Computer Science
Aalto University
mohsen.amidzade@aalto.fi

Abstract

Stochastic Optimal Control Problems (SOCPs) plays a major role in the sequential decision-making challenges. There exist various iterative algorithms, under framework of stochastic maximum principle, that sequentially find the optimal control decision. However, they are based on the adjoint sensitivity analysis that necessitates simulation of an adjoint process — typically a backward stochastic differential equation (SDE) that must simultaneously be adapted to a forward filtration and satisfy a terminal condition — which substantially increases complexity and exacerbates the curse of dimensionality. We instead develop a stochastic maximum principle based on the Malliavin calculus, which enables us to devise an iterative algorithm without need of an adjoint process. Our algorithm however needs the Malliavin derivative that can be efficiently computed based on a forward simulator. Empirical comparisons against standard iterative algorithms demonstrate that our approach alleviates the dimensionality bottleneck while delivering competitive performance on the considered SOCPs.

1 Introduction

Stochastic optimal control problems (SOCPs) stand as a vibrant research domain presenting extensive applications across various fields such as nonlinear filtering, game theory, and mathematical finance (Ma & Yong, 1999; Zhang, 2017, 2022; Bouchard et al., 2018; Hientzsch, 2019). These problems are characterized by functional objectives depending on diffusion processes generated from stochastic differential equations (SDEs).

There are two main frameworks that characterize the optimal solution of SOCPs, namely Stochastic Maximum Principle (SMP) and Hamilton-Jacobi-Bellman (HJB) equations (Yong & Zhou, 1999). Under the framework of SMP, there are various iterative algorithms that find the optimal control decision. Gong et al. (2017) leverages a gradient projection method to develop an iterative algorithm based on the adjoint sensitivity analysis. Specifically, their approach needs simulation of an adjoint process (or a backward SDE) that must simultaneously be adapted to a forward filtration and complies with a terminal condition. This requirement challenges the solution methodology; the available mechanisms need extensive computations and suffer from the curse of dimensionality (Archibald et al., 2020). A remedy for this challenge is to approximate the adjoint process based on a time-reversed computation Archibald et al. (2020); Wang & Liu (2025). Although, this approximating method is computationally effective, but it cannot give the exact solution and sometimes needs extra iteration updates to converge. Conversely, our paper develops a SMP based on the Malliavin calculus, and accordingly a gradient projection algorithm, termed as Mal-GPro. In contrast to the aforementioned approaches, our algorithm does not need an additional adjoint process, and more importantly is accurate from this sense that it does not use any approximation. Our algorithm manages to replace the adjoint state with the Malliavin derivative of the original SDE that can be computed based on a forward simulator.

This paper thus provides the following contributions.

- We derive a stochastic maximum principle for vector (and scalar) SOCPs relying on the Malliavin calculus. We then derive optimality conditions for the optimal control decision.
- Based on the developed framework, we devise a gradient projection algorithm replacing the adjoint state with a Malliavin derivative, that iteratively find the optimal solution for some classes of SOCPs.
- We benchmark our algorithm against other iterative algorithms using numerous experiments, which shows the effectiveness of our algorithm from dimensionality bottleneck and performance perspectives.

2 Related Work

Sensitivity analysis-based methods: Our work has some connections with the sensitivity analysis works that leverage the Malliavin calculus. Gobet & Munos (2005) performs a sensitivity analysis for stochastic objectives depending on the final solution of a (controlled) SDE. Meyer-Brandis et al. (2012) derives a stochastic maximum principle framework for *scalar* SOCPs based on the Malliavin calculus. In contrast, we consider more general forms of vector SOCPs, and more importantly, we devise an iterative projection algorithm to obtain the optimal control decision.

Iterative gradient algorithms: Gradient algorithms manage to find the control decision for SOCPs based on the framework of SMP. A gradient projection method has been developed in (Gong et al., 2017) based on the adjoint backward SDE. The adjoint state should be adapted to a forward Wiener filtration and follow the terminal condition. Therefore, the available solutions to simulate this SDE, either mesh-based non-parametric or mesh-free parametric methods, suffer from the curse of dimensionality (Archibald et al., 2020). Accordingly, an approximate solution has been proposed in Archibald et al. (2020); Wang & Liu (2025) to simulate the backward SDE based on a time-reversed computation. However, the solution exhibits an approximation which suffers from the performance drop. In contrast, our proposed algorithm replaces the backward adjoint SDE with a Malliavin derivative that does not require backward simulation. More importantly, it does not rely on any approximation to simulate the Malliavin derivative.

3 Background

3.1 Variational Analysis of SOCPs

In this paper, we consider the filtered probability space $(\Omega, \mathcal{F}, \mathcal{P})$, where Ω is the sample space, \mathcal{F} the σ -algebra event space, and $\mathcal{P} : \mathcal{F} \rightarrow [0, 1]$ the probability measure. A l -dimensional Wiener process $\mathbf{W} = \{w_t^l\}_{l=1}^d$ with diffusion matrix $\mathbf{Q} = [q_{i,j}]_{i,j}$ is then defined with the natural filtration $\mathcal{F}_t \subseteq \mathcal{F}$ that encodes all information up to time t .

We now consider the following controlled SDE:

$$\begin{cases} d\mathbf{x}_t^{\mathbf{u}} = \mathbf{a}(\mathbf{x}_t^{\mathbf{u}}, \mathbf{u}_t) dt + \sum_{i=1}^l \mathbf{b}_i(\mathbf{x}_t^{\mathbf{u}}, \mathbf{u}_t) dw_t^i, \\ \mathbf{x}_0 \text{ given} \end{cases} \quad (1)$$

where $\mathbf{x}_t^{\mathbf{u}} \in \mathbb{R}^n$ is the process, $\mathbf{a} : \mathbb{R}^n \times U \rightarrow \mathbb{R}^n$ is the drift function which describes the dynamics of the SDE and is governed by a \mathcal{F}_t -adapted control process $\mathbf{u}_t \in U$, with U an open convex set in \mathbb{R}^k , $\mathbf{b}_i : \mathbb{R}^n \times U \rightarrow \mathbb{R}^n$ is the diffusion function determining the extent of uncertainty added to the dynamics, and $\mathbf{B} = [\mathbf{b}_1, \dots, \mathbf{b}_d]$. Hereafter, we may use the notation \mathbf{x}_t , instead of $\mathbf{x}_t^{\mathbf{u}}$, for the simplicity. A cost functional pertaining to this SDE is then considered as follows:

$$J(\mathbf{u}, \mathbf{x}_0) = \mathbb{E} \left\{ \int_0^T L(\mathbf{x}_t^{\mathbf{u}}, \mathbf{u}_t, t) dt + h(\mathbf{x}_T^{\mathbf{u}}) \right\}, \quad (2)$$

where $L : \mathbb{R}^n \times U \times [0, T] \rightarrow \mathbb{R}$ and $h^f : \mathbb{R}^n \rightarrow \mathbb{R}$ are some measurable functions. The stochastic control problem of interest is then formulated as:

$$\begin{aligned} P_1 : \max_{\mathbf{u} \in U} J(\mathbf{u}, \mathbf{x}_0) \\ \text{s.t. } d\mathbf{x}_t = \mathbf{a}(\mathbf{x}_t, \mathbf{u}_t) dt + \sum_{i=1}^l \mathbf{b}_i(\mathbf{x}_t, \mathbf{u}_t) dw_t^i. \end{aligned} \quad (3)$$

A perturbation analysis is then employed to find the optimal control of SOCP P_1 . For this, the control $\mathbf{u}_t \in U$ is perturbed through $\mathbf{u}_t + \epsilon \mathbf{v}_t$, and then the variation of functional (2) is analyzed along direction \mathbf{v}_t based on the following definition.

Definition 3.1. The variation of functional $J(\mathbf{u}, \mathbf{x}_0)$ along direction \mathbf{v}_t is:

$$\delta_{\mathbf{v}} J(\mathbf{u}, \mathbf{x}_0) = \lim_{\epsilon \rightarrow 0} \frac{1}{\epsilon} (J(\mathbf{u} + \epsilon \mathbf{v}, \mathbf{x}_0) - J(\mathbf{u}, \mathbf{x}_0))$$

This definition shows how the functional $J(\mathbf{u}(\cdot), \cdot)$ evolves by slightly perturbing the process $\mathbf{u}(\cdot)$. Using this definition, one can have:

Proposition 3.2. Consider SOCP P_1 with the cost functional $J(\mathbf{u}, \mathbf{x}_0)$ (2), its variation along the direction $\mathbf{v}(\cdot)$ is obtained by:

$$\delta_{\mathbf{v}} J(\mathbf{u}, \mathbf{x}_0) = \mathbb{E} \left\{ \int_0^T H_{\mathbf{u}}(\mathbf{x}, \mathbf{y}, \mathbf{u}, \mathbf{Z}, t)^\top \mathbf{v}_t dt \right\},$$

where $H_{\mathbf{u}}$ is the gradient of the Hamiltonian H w.r.t. \mathbf{u}_t with

$$H(\mathbf{x}, \mathbf{y}, \mathbf{u}, \mathbf{Z}, t) := L(\mathbf{x}_t, \mathbf{u}_t, t) + \mathbf{a}(\mathbf{x}_t, \mathbf{u}_t)^\top \mathbf{y}(t) + \sum_{i=1}^l \mathbf{b}_i(\mathbf{x}_t, \mathbf{u}_t)^\top \mathbf{z}_t^i,$$

and $\mathbf{y}_t \in \mathbb{R}^n$ is an adjoint process which is obtained based on the following backward SDE:

$$\begin{cases} d\mathbf{y}_t &= -H_{\mathbf{x}}(\mathbf{x}, \mathbf{y}, \mathbf{u}, \mathbf{Z}, t) dt + \sum_{i=1}^l \mathbf{z}_t^i dw_t^i \\ \mathbf{y}_T &= \nabla_{\mathbf{x}(t)} h(\mathbf{x}_T), \end{cases} \quad (4)$$

with $\mathbf{z}^i \in \mathbb{R}^n$ being a control process associated to the adjoint process \mathbf{y} where $\mathbf{z}_t^i = \mathcal{J}_{\mathbf{x}(t)} \mathbf{y}_t^\top \mathbf{b}_i(\mathbf{x}_t, \mathbf{u}_t)$, $\mathbf{Z} = \{\mathbf{z}^i\}_{i=1}^l$, and $H_{\mathbf{x}}$ is the gradient of H w.r.t. \mathbf{x} .

Proof. Please refer to (Yong & Zhou, 1999; Geng et al., 2021) for the proof. \square

Definition 3.3. The control process \mathbf{u}^* is called a critical decision for problem P_1 , if $\delta_{\mathbf{v}} J(\mathbf{u}^*, \mathbf{x}_0) = 0$ through the perturbation $\mathbf{u}^* + \epsilon \mathbf{v}$ for any \mathcal{F}_t -adapted process $\mathbf{v}_t \in U$.

Iterative algorithm: For deterministic control decisions, a gradient projection method can be established to find the optimum solution \mathbf{u} (Archibald et al., 2020; Wang & Liu, 2025). This method utilizes the following update rule:

$$\mathbf{u} \leftarrow P \left(\mathbf{u} + \lambda \mathbb{E} \{ H_{\mathbf{u}}(\mathbf{x}, \mathbf{y}, \mathbf{u}, \mathbf{Z}, t) \} \right), \quad (5)$$

where λ is the learning rate and $P(\cdot)$ is a projection operator to U .

3.2 Malliavin Calculus

Malliavin derivative is a tool in the stochastic analysis that capture the sensitivity of processes with respect to the variations of Wiener process $\mathbf{W} = (w_s)_{s \in [0, t]}$. Assume process $x_t = \int_0^t g_t dw_t$ for deterministic function g_t , then its Malliavin derivative against w_s , denoted by $D_s x_t$, is defined to be $D_s x_t = g_s$ for all $s \leq t$. The chain rule also holds for this derivative, implying that for an adapted process u_t and a smooth functional $F(\cdot)$ in the domain of the Malliavin derivative, we can get $D_s F(u_t) = \frac{\partial F(u_t)}{\partial u_t} D_s u_t$. We also need to mention the integration-by-parts formula in the Malliavin

calculus (Alòs & García Lorite, 2021; Nualart & Nualart, 2018), which plays a vital role in this work. It states that for the functional $F(\cdot)$ and any adapted process u_s with square-integrability, one can get

$$\mathbb{E}\left\{F \int_0^t u_s dw_s\right\} = \mathbb{E}\left\{\int_0^t D_s F u_s ds\right\}. \quad (6)$$

We also need to mention the Malliavin derivative of a diffusion process. For this, consider the n -dimensional SDE

$$\text{SDE}(\mathbf{a}, \mathbf{B}, \mathbf{x}_0) : d\mathbf{x}_t = \mathbf{a}(\mathbf{x}_t, t)dt + \sum_{l=1}^d \mathbf{b}_l(\mathbf{x}_t, t)dw_t^l \quad (7)$$

with $\mathbf{a} : \mathbb{R}^n \times [0, T] \rightarrow \mathbb{R}^n$ and $\mathbf{B} = [\mathbf{b}_1, \dots, \mathbf{b}_d] : \mathbb{R}^n \times [0, T] \rightarrow \mathbb{R}^{n \times d}$ being measurable functions with bounded partial derivatives. Then, the Malliavin derivative of \mathbf{x}_t against w_s^i follows (Nualart & Nualart, 2018):

$$D_s^i \mathbf{x}_t = \mathbf{b}_i(\mathbf{x}_t) + \sum_{l=1}^d \int_s^t \mathcal{J}_{\mathbf{x}} \mathbf{b}_l(\mathbf{x}_\tau) D_s^i \mathbf{x}_\tau dw_\tau^l + \int_s^t \mathcal{J}_{\mathbf{x}} \mathbf{a}(\mathbf{x}_\tau) D_s^i \mathbf{x}_\tau d\tau, \quad i \in \{1, \dots, d\}. \quad (8)$$

Moreover, the Malliavin matrix $D_s \mathbf{x}_t = [D_s^1 \mathbf{x}_t, \dots, D_s^d \mathbf{x}_t]$ follows (Nualart & Nualart, 2018)

$$D_s \mathbf{x}_t = \mathbf{\Gamma}_{s,t} \mathbf{B}(\mathbf{x}_s, s), \quad (9)$$

where $\mathbf{\Gamma}_{s,t} = \mathbf{Y}_t \mathbf{Z}_s$, and the matrix-valued stochastic flows $\mathbf{Y}_t = \frac{\partial \mathbf{x}_t}{\partial \mathbf{x}_0} \in \mathbb{R}^{n \times n}$ and $\mathbf{Z}_t = \mathbf{Y}_t^{-1} \in \mathbb{R}^{n \times n}$ comply with the following variational SDEs:

$$\begin{aligned} \mathbf{Y}_t &= \mathbf{I} + \sum_{l=1}^d \int_0^t \mathcal{J}_{\mathbf{x}} \mathbf{b}_l(\mathbf{x}_s, s) \mathbf{Y}_s dw_s^l + \int_0^t \mathcal{J}_{\mathbf{x}} \mathbf{a}(\mathbf{x}_s, s) \mathbf{Y}_s ds \\ \mathbf{Z}_t &= \mathbf{I} - \sum_{l=1}^d \int_0^t \mathbf{Z}_s \mathcal{J}_{\mathbf{x}} \mathbf{b}_l(\mathbf{x}_s, s) dw_s^l - \int_0^t \mathbf{Z}_s \left(\mathcal{J}_{\mathbf{x}} \mathbf{a}(\mathbf{x}_s, s) - \sum_{l=1}^d \mathcal{J}_{\mathbf{x}} \mathbf{b}_l(\mathbf{x}_s, s)^2 \right) ds. \end{aligned} \quad (10)$$

It is noteworthy that the Malliavin derivative has the following expression for the scalar case, (i.e., $n = d = 1$):

$$D_s x_t = b(x_s, s) \exp \left(\int_s^t (a_x(x_t, t) - \frac{1}{2} b_x(x_t, t)^2) dt + \int_s^t b_x(x_t, t) dw_t \right), \quad \text{for } s \leq t. \quad (11)$$

4 Variational Analysis of SOCPs using Malliavin Calculus

Proposition (3.2) find the variation of the cost functional of SOCP P_1 based on an adjoint state governed by a backward SDE. However, solving a backward SDE should lead to a process \mathbf{y}_t that should at the same time satisfy the terminal condition $\mathbf{y}_T = \nabla_{\mathbf{x}(t)} h(\mathbf{x}_T)$ and be \mathcal{F}_t -adapted. This requirement makes the solution methodologies challenging (Chessari et al., 2023). Instead, we intend to develop a variational framework for SOCP P_1 based on the Malliavin calculus that can provide a more efficient solution approach.

Scalar Scenario:

In this section, we concentrate on a scalar case of SOCP P_1 , where $n = k = 1$. This indeed gives an intuition for the general case where we have a vector problem. In this regard, we consider the following theorem.

Theorem 4.1. *Consider SOCP P_1 (3) with $n = k = 1$, the variation of cost functional $J(u, x_0)$ along direction v , with perturbation $u + \epsilon v$, can be obtained by:*

$$\begin{aligned} \delta_v J(u, x_0) &= \mathbb{E} \int_0^T \left\{ \frac{a_u(s) - b_x(s) b_u(s)}{b(s)} \left(\int_s^T L_x(t) D_s x_t dt + h_x(x_T) D_s x_T \right) \right. \\ &\quad \left. + \frac{b_u(s)}{b(s)} \left(\int_s^T (L_{xx}(t) D_s x_t + L_{xu}(t) D_s u_t) D_s x_t dt + h_{xx}(x_T) D_s x_T^2 \right) + L_u(s) \right\} v_s ds, \end{aligned} \quad (12)$$

where $D_s x_t$ (respectively, $D_s u_t$) is the Malliavin derivative of x_t (respectively, u_t) against w_s , $L_x(t)$, $a_u(s)$, and $b(s)$ are short notations for $L_x(x_t, u_t, t)$, $a_u(x_s, u_s)$ and $b(x_s, u_s)$, respectively, with L_x and L_{xx} denoting the first and second gradients of L w.r.t x , and L_u , a_u , b_u showing the gradient of L , a and b w.r.t. u .

Proof. Please refer to Section A. \square

We need to highlight that the presence of $b(s)$ in the denominators of Equation (12) is not problematic, as $\frac{D_s x_t}{b(s)}$ exists for $t \in [0, T]$. Variation analysis in Theorem 4.1 does not rely on any adjoint process, in contrast to Proposition (3.2) which depends on adjoint state \mathbf{y}_t as well as on control process $\{\mathbf{z}_t^i\}_{i=1}^d$ (see Equation (4)). However, Theorem 4.1 needs computation of the Malliavin derivative of the diffusion process, i.e., $D_s x_t$, which can be computed through an efficient and time-reversed mechanism without involving new process (see Section 5.2).

Corollary 4.2. Consider u^* be a critical point for $J(u, x_0)$ of problem P_1 , i.e., $\delta_v J(u^*, x_0) = 0$ through the perturbation $u^* + \epsilon v$, then we have:

$$\begin{aligned} \mathbb{E} \left\{ \frac{a_u(s) - b_x(s)b_u(s)}{b(s)} \left(\int_s^T L_x(t) D_s x_t^* dt + h_x(x_T^*) D_s x_T^* \right) \right. \\ \left. + \frac{b_u(s)}{b(s)} \left(\int_s^T (L_{xx}(t) D_s x_t^* + L_{xx}(t) D_s u_t^*) D_s x_t^* dt + h_{xx}(x_T^*) D_s x_T^{*2} \right) + L_u(s) \middle| \mathcal{F}_s \right\} = 0, \end{aligned} \quad (13)$$

where $x_t^* = x_t^{u^*}$

Proof. It follows from this fact that Equation (12) holds for every \mathcal{F}_s -adapted process v_s . \square

Vector Scenario: The following theorem obtains a variation of SOCP P_1 in the general case of vector problems based on the Malliavin calculus.

Theorem 4.3. Consider SOCP P_1 (3), the variation of cost functional $J(\mathbf{u}, \mathbf{x}_0)$ along direction \mathbf{v} , with perturbation $\mathbf{u} + \epsilon \mathbf{v}$, can be obtained by:

$$\begin{aligned} \delta_v J(\mathbf{u}, \mathbf{x}_0) = \mathbb{E} \int_0^T \left\{ \left(\int_s^T \nabla_x L(t)^\top \Gamma_{s,t} dt + \nabla_x h(\mathbf{x}_T)^\top \Gamma_{s,T} \right) \left(\mathcal{J}_u \mathbf{a}(s) - \sum_{l,l'}^d q_{l,l'} \mathcal{J}_x \mathbf{b}_l(s) \mathcal{J}_u \mathbf{b}_{l'}(s) \right) \right. \\ \left. + \sum_{l=1}^d \left(\int_s^T (D_s^l \mathbf{x}_t^\top \nabla_x^2 L(t) + D_s^l \mathbf{u}_t^\top \nabla_{ux} L(t)) \Gamma_{s,t} dt + D_s^l \mathbf{x}_T^\top \nabla_x^2 h(\mathbf{x}_T) \Gamma_{s,T} \right) \mathcal{J}_u \mathbf{b}_l(s) \right. \\ \left. + \nabla_u L(s)^\top \right\} \mathbf{v}_s ds, \end{aligned}$$

where $D_s^l \mathbf{x}_t$ (respectively, $D_s^l \mathbf{u}_t$) is the Malliavin derivative of \mathbf{x}_t (respectively, \mathbf{u}_t) against w_t^l , $\mathbf{Q} = [q_{i,j}]_{ij}$ is the diffusion matrix of Wiener process with $q_{l,l'}$ the diffusion coefficient between w_t^l and $w_t^{l'}$, $\Gamma_{s,t}$ relates to the Malliavin derivative $D_s \mathbf{x}_t$ through Equation (9) (i.e., $D_s \mathbf{x}_t = \Gamma_{s,t} \mathbf{B}(\mathbf{x}_s, s)$), and $\mathcal{J}_x \mathbf{a}$ (respectively, $\mathcal{J}_u \mathbf{a}$) stands for the Jacobian matrix of vector \mathbf{a} w.r.t. \mathbf{x} (respectively, \mathbf{u}).

Proof. Please refer to Section B. \square

Again, we compare the variation analysis of Theorem 4.3 to that of Proposition (3.2). The former does not depend on any adjoint process, while the latter does. However, Theorem 4.3 need computation of stochastic flow $\Gamma_{s,t}$ pertaining to the Malliavin derivative through Equation (9), which can be computed efficiently using the approach presented in Section 5.2.

Corollary 4.4. Consider \mathbf{u}^* be a critical point for $J(\mathbf{u}, \mathbf{x}_0)$ of problem P_1 , i.e., $\delta_v J(\mathbf{u}^*, \mathbf{x}_0) = 0$ through the perturbation $\mathbf{u}^* + \epsilon \mathbf{v}$, we then have:

$$\begin{aligned} \mathbb{E} \left\{ \left(\int_s^T \nabla_x L(t)^\top \Gamma_{s,t}^* dt + \nabla_x h(\mathbf{x}_T^*)^\top \Gamma_{s,T}^* \right) \left(\mathcal{J}_u \mathbf{a}(s) - \sum_{l,l'}^d q_{l,l'} \mathcal{J}_x \mathbf{b}_l(s) \mathcal{J}_u \mathbf{b}_{l'}(s) \right) \right. \\ \left. + \sum_{l=1}^d \left(\int_s^T (D_s^l \mathbf{x}_t^{* \top} \nabla_x^2 L(t) + D_s^l \mathbf{u}_t^{* \top} \nabla_{ux} L(t)) \Gamma_{s,t}^* dt + D_s^l \mathbf{x}_T^{* \top} \nabla_x^2 h(\mathbf{x}_T^*) \Gamma_{s,T}^* \right) \mathcal{J}_u \mathbf{b}_l(s) \right. \\ \left. + \nabla_u L(s)^\top \middle| \mathcal{F}_s \right\} = 0, \end{aligned} \quad (14)$$

where $\mathbf{x}_t^* = \mathbf{x}_t^{u^*}$ and $D_s \mathbf{x}_t^* = \Gamma_{s,t}^* \mathbf{B}(\mathbf{x}_s^*, s)$.

5 An Iterative Approach for SOCPs based on Malliavin Calculus

In this section, we intend to develop a gradient projection algorithm to solve SOCPs with deterministic control decision $\mathbf{u} \in \mathcal{U}$, where \mathcal{U} here is a nonempty convex set whose elements are square-integrable. For this purpose, we first find an expression for the Gateaux derivative (Gong et al., 2017) of cost functional $J(\mathbf{u}, \mathbf{x}_0)$, and then outline a fixed-point scheme for optimizing the control decision \mathbf{u} . Accordingly, we manage to devise an iterative algorithm to solve SOCP P_1 .

We now need to draw the following remark.

Remark 5.1. For SOCP P_1 (3) with deterministic control decision $\mathbf{u} \in \mathcal{U}$, Theorem 4.1 (respectively, Theorem 4.3) provides a representation for the Gateaux derivative of cost functional $J(u, x_0)$ (respectively, $J(\mathbf{u}, \mathbf{x}_0)$) with respect to the control decision at $t = s$ (Gong et al., 2017):

$$J'(u, x_0)|_s = \mathbb{E} \left\{ \frac{a_u(s) - b_x(s)b_u(s)}{b(s)} \left(\int_s^T L_x(t) D_s x_t dt + h_x(x_T) D_s x_T \right) + \frac{b_u(s)}{b(s)} \left(\int_s^T L_{xx}(t) D_s x_t^2 dt + h_{xx}(x_T) D_s x_T^2 \right) + L_u(s) \right\} \quad (15)$$

and

$$\begin{aligned} \nabla_{\mathbf{u}} J(\mathbf{u}, \mathbf{x}_0)|_s = \mathbb{E} \left\{ \left(\int_s^T \nabla_{\mathbf{x}} L(t)^\top \Gamma_{s,t} dt + \nabla_{\mathbf{x}} h(\mathbf{x}_T)^\top \Gamma_{s,T} \right) \left(\mathcal{J}_{\mathbf{u}} \mathbf{a}(s) - \sum_{i,l'} q_{i,l'} \mathcal{J}_{\mathbf{x}} \mathbf{b}_l(s) \mathcal{J}_{\mathbf{u}} \mathbf{b}_{l'}(s) \right) \right. \\ \left. + \sum_{l=1}^d \left(\int_s^T [\Gamma_{s,t} \mathbf{B}(s)]_l^\top \nabla_{\mathbf{x}}^2 L(t) \Gamma_{s,t} dt + [\Gamma_{s,T} \mathbf{B}(s)]_l^\top \nabla_{\mathbf{x}}^2 h(\mathbf{x}_T) \Gamma_{s,T} \right) \mathcal{J}_{\mathbf{u}} \mathbf{b}_l(s) \right. \\ \left. + \nabla_{\mathbf{u}} L(s)^\top \right\}. \quad (16) \end{aligned}$$

Having obtained the Gateaux derivative based on Remark 5.1, we can outline a gradient projection method inspired by the scheme (5). Specifically, for scalar SOCPs, we set the following update rule:

$$u^{i+1} \leftarrow \mathbf{P} \left(u^i + \lambda J'(u^i, x_0) \right), \quad (17)$$

and for vector SOCPs:

$$\mathbf{u}^{i+1} \leftarrow \mathbf{P} \left(\mathbf{u}^i + \lambda \nabla_{\mathbf{u}} J(\mathbf{u}^i, \mathbf{x}_0) \right), \quad (18)$$

where i is the iteration index.

In the sequel, we aim to numerically implement the gradient projection iteration in Equations (17) and (18). To accomplish this goal, we need to (i) apply a discretization method on the gradient projection, (ii) compute the stochastic flow $\Gamma_{s,t}$ and Malliavin derivative $D_s \mathbf{x}_t$ in Equations (15) and (16), and (iii) accordingly develop a numerical iterative algorithm to solve SOCP P_1 .

5.1 Numerical Implementation of Gradient Projection

We here discretize the gradient projection scheme. Accordingly, we first partition the interval $[0, T]$ based on N fixed sub-intervals $\Pi_N := \{[t_{j-1}, t_j]\}_{j=1}^N$, where $t_0 = 0$, $t_N = T$ and $\Delta t := t_j - t_{j-1} = \frac{T}{N}$ is the duration of each sub-interval. Accordingly, the piece-wise control decision can be obtained by \mathbf{u}_{t_j} for $j \in \{1, \dots, N\}$. We then apply this discretization policy for the gradient projection scheme (17)-(18) to get:

$$\begin{aligned} u_{t_j}^{i+1} &\leftarrow \mathbf{P}_N \left(u_{t_j}^i + \lambda J'^N(u^i, x_0)|_{t_j} \right), \\ \mathbf{u}_{t_j}^{i+1} &\leftarrow \mathbf{P}_N \left(\mathbf{u}_{t_j}^i + \lambda \nabla_{\mathbf{u}} J^N(\mathbf{u}^i, \mathbf{x}_0)|_{t_j} \right), \quad \text{for } j \in \{1, \dots, N\} \end{aligned} \quad (19)$$

where $\mathbf{u}_{t_j}^i$ is the discrete approximation of \mathbf{u}_{t_j} at iteration i , J'^N (respectively, $\nabla_{\mathbf{u}} J^N$) is the discrete approximation of J' (respectively, $\nabla_{\mathbf{u}} J$), and $\mathbf{P}_N(\cdot)$ is an operator that projects onto the set \mathcal{U}_N with

$$\mathcal{U}_N = \left\{ \mathbf{u} \in \mathcal{U} \mid \mathbf{u} = \sum_{j=1}^N \alpha_j I_{[t_{j-1}, t_j]}, \alpha_j \in \mathbb{R}^k \right\}.$$

The following theorem then studies the convergence of the gradient projection scheme (19); Note that we present this theorem merely for the vector SOCPs, the scalar version can be simply derived.

Algorithm 1: Computation of Stochastic Flow $\Gamma_{s,t}$ and Malliavin Derivative $D_s \mathbf{x}_t$

Data: Forward trajectory $(\mathbf{x}_r, \mathbf{w}_r)$, time-step Δt .
// Initialize via terminal condition:
 $\Gamma_{r,r} \leftarrow \mathbf{I}$
// Solve the SDE (21):
for $t \leftarrow r$ to T with step Δt do
 Compute $\Delta \Gamma_{r,t} = \left(\mathcal{J}_x \mathbf{a}(\mathbf{x}_t, \mathbf{u}_t) \Delta t + \sum_{l=1}^d \mathcal{J}_x \mathbf{b}_l(\mathbf{x}_t, \mathbf{u}_t) (\mathbf{w}_t - \mathbf{w}_{t-\Delta t}) \right) \Gamma_{r,t}$
 Update $\Gamma_{r,t+\Delta t} \leftarrow \Gamma_{r,t} + \Delta \Gamma_{r,t}$
// Recover Malliavin derivatives:
for $t \in \{r, r + \Delta t, \dots, T\}$ do
 $D_r \mathbf{x}_t \leftarrow \Gamma_{r,t} \mathbf{B}(\mathbf{x}_r, r)$
return $\Gamma_{r,t}$ and $D_r \mathbf{x}_t$ for $t \in \{r, r + \Delta t, \dots, T\}$

Theorem 5.2. Denote $\mathbf{u}^{*,N}$ as the fixed-point solution of the projection scheme (19), i.e., $\mathbf{u}^{*,N} = \mathbf{P}_N(\mathbf{u}^{*,N} + \lambda \nabla_{\mathbf{u}} J^N(\mathbf{u}^{*,N}, \mathbf{x}_0))$. Further, assume $\nabla_{\mathbf{u}} J(\mathbf{u}, \mathbf{x}_0)$ is Lipschitz continuous with the constant L around \mathbf{u}^* and $\mathbf{u}^{*,N}$, i.e.,

$$\|\nabla_{\mathbf{u}}(\mathbf{u}^*, \mathbf{x}_0) - \nabla_{\mathbf{u}}(\mathbf{u}, \mathbf{x}_0)\| \leq L \|\mathbf{u}^* - \mathbf{u}\|, \quad \forall \mathbf{u} \in \mathcal{U},$$

$$\|\nabla_{\mathbf{u}}(\mathbf{u}^{*,N}, \mathbf{x}_0) - \nabla_{\mathbf{u}}(\mathbf{u}, \mathbf{x}_0)\| \leq L \|\mathbf{u}^{*,N} - \mathbf{u}\|, \quad \forall \mathbf{u} \in \mathcal{U}_N$$

and uniformly monotone with the rate r around \mathbf{u}^* and $\mathbf{u}^{*,N}$, i.e.,

$$(\nabla_{\mathbf{u}}(\mathbf{u}^*, \mathbf{x}_0) - \nabla_{\mathbf{u}}(\mathbf{u}, \mathbf{x}_0))^\top (\mathbf{u}^* - \mathbf{u}) \geq r \|\mathbf{u}^* - \mathbf{u}\|^2, \quad \forall \mathbf{u} \in \mathcal{U},$$

$$(\nabla_{\mathbf{u}}(\mathbf{u}^{*,N}, \mathbf{x}_0) - \nabla_{\mathbf{u}}(\mathbf{u}, \mathbf{x}_0))^\top (\mathbf{u}^{*,N} - \mathbf{u}) \geq r \|\mathbf{u}^{*,N} - \mathbf{u}\|^2, \quad \forall \mathbf{u} \in \mathcal{U}_N,$$

Moreover, $\nabla_{\mathbf{u}} J^N$ tends to $\nabla_{\mathbf{u}} J$ as $N \rightarrow \infty$, and λ is chosen such that $0 < 1 - 2r\lambda + (1+2L)\lambda^2 < \delta^2$ with $\delta \in (0, 1)$. Then, the discrete approximation of control decision complies with the following bound as $i \rightarrow \infty$:

$$\|\mathbf{u}^* - \mathbf{u}^i\| \sim \mathcal{O}(\Delta t).$$

Proof. It can be proved by following the procedure of Theorem 3.1 in (Gong et al., 2017). \square

The next section explains how the stochastic flow and Malliavin derivative required for the Gateaux derivative $\nabla_{\mathbf{u}} J(\mathbf{u}, \mathbf{x}_0)$ can be computed.

5.2 Computation of Stochastic Flow and Malliavin Derivative

The Gateaux derivative in Remark 5.1 depends on the stochastic flow $\Gamma_{s,t}$ (or Malliavin derivative $D_s \mathbf{x}_t$). Here, we intend to leverage an approach to compute this information. In this regard, we need to first present the following proposition.

Proposition 5.3. Consider the Malliavin derivative $D_r \mathbf{x}_t = [D_r^1 \mathbf{x}_t, \dots, D_r^d \mathbf{x}_t]$ (8) of SDE (1), we have

$$D_r \mathbf{x}_t = \Gamma_{r,t} \mathbf{B}(\mathbf{x}_r, r), \quad \text{for } r \leq t, \quad (20)$$

where $\Gamma_{r,t} \in \mathbb{R}^{n \times n}$ represents a linear SDE, and adapted to the filtration \mathcal{F}_r obtained by:

$$\text{SDE}(\mathcal{J}_x \mathbf{a}, \mathcal{J}_x \mathbf{B}, \Gamma_{r,r} = \mathbf{I}) : d\Gamma_{r,t} = \left(\sum_{l=1}^d \mathcal{J}_x \mathbf{b}_l(\mathbf{x}_t, \mathbf{u}_t) dw_t^l + \mathcal{J}_x \mathbf{a}(\mathbf{x}_t, \mathbf{u}_t) dt \right) \Gamma_{r,t}, \quad (21)$$

with initial condition $\Gamma_{r,r} = \mathbf{I}$

Proof. see Section C. \square

Proposition 5.3 together with an SDE-simulator provide a method to recursively compute the Malliavin derivative $D_r \mathbf{x}_t$. Specifically, for each $t \in [0, T]$, this approach starts from the initial condition $\Gamma_{r,r} = \mathbf{I}$, gradually increments the parameter t , and computes the right hand side of Equation (21). Algorithm 1 shows pseudo-code based on the Euler-Maruyama scheme with a convergence rate proportional to $\sqrt{\Delta t}$ (Kloeden & Platen, 1992).

Algorithm 2: Gradient Projection Algorithm based on Malliavin Calculus (Mal-GPro)

Input: Initial state \mathbf{x}_0 ,
Output: Optimal control process \mathbf{u} .
for $i = 1$ **to** N_{eps} **do**
 // Simulate the SDE (7) within the partition Π_N via any SDE solver
 $(\mathbf{x}_t, \mathbf{w}_t) \leftarrow \text{SDEsolve}(\mathbf{a}, \mathbf{B}, \mathbf{x}_0), t \in \Pi_N$;
 // Compute Stochastic flow $\Gamma_{s,t}$ and Malliavin derivative $D_s x_t$ by
 solving SDE (21) using Algorithm 1:
 $(\Gamma_{s,t}, D_s \mathbf{x}_t) \leftarrow \text{SDEsolve}(\mathcal{J}_x \mathbf{a}, \mathcal{J}_x \mathbf{B}, \Gamma_{t,t}), s \in \Pi_N, t \in \Pi_N, s \leq t$;
 // Compute the functional gradient based on the SOCP problem:
 if scalar then
 compute $J'^N(u, x_0)|_t$ via Equation (15).
 else
 compute $\nabla_{\mathbf{u}} J^N(\mathbf{u}, \mathbf{x}_0)|_t$ via Equation (16).
 // Update control process via the projection gradient (19):
 if scalar then
 $u_t^{i+1} \leftarrow P_N(u_t^i + \lambda J'^N(u^i, x_0)|_t), \text{ for } t \in \Pi_N$.
 else
 $\mathbf{u}_t^{i+1} \leftarrow P_N(\mathbf{u}_t^i + \lambda \nabla_{\mathbf{u}} J^N(\mathbf{u}^i, \mathbf{x}_0)|_t), \text{ for } t \in \Pi_N$.

5.3 A Gradient Projection Algorithm via Malliavin Calculus

The materials of Sections 5.1 and 5.2 enables us to present an iterative mechanism for solving SOCP P_1 . We accordingly devise a projection algorithm based on the numerical scheme in Equation (19), Theorem 5.1 and Algorithm 1. As this algorithm is based on a gradient projection approach utilizing Malliavin calculus, we term it as Mal-GPro. This algorithm includes 3 main phases as follows.

- **Forward Pass:** SDE (7) is simulated within discrete partition Π_N using any SDE-solver, e.g. Euler-Maruyama one, to obtain the stochastic paths $(\mathbf{x}_t, \mathbf{W}_t)_{t \in \Pi_N}$. Additionally, we compute the stochastic flow and Malliavin derivatives $(\Gamma_{s,t}, D_s \mathbf{x}_t)_{t \in \Pi_N, s \in \Pi_N}$ with $s \leq t$ using Algorithm 1.
- **Gradient Computation:** the discrete gradient of cost functional $\nabla_{\mathbf{u}} J^N(\mathbf{u}, \mathbf{x}_0) / J'^N(u, \mathbf{x}_0)$ is computed according to Remark 5.1 and using Equations (15) and (16).
- **Update Control:** the control process is then updated via the projection gradient approach Equation (19) with learning rate λ .

The pseudo-code of this algorithm is presented in Algorithm 2.

6 State-of-the-Art Algorithms from Literature

We compare the performance of Mal-GPro algorithm with two adjoint-based algorithms derived based on the stochastic maximum principle with adjoint sensitivity mechanism. They are explained as follows.

6.1 Gradient Projection Method

This algorithm is established based on the variational analysis presented in Section 3.1, and follows the update mechanism in Equation (5) (Gong et al., 2017). In this regard, two \mathcal{F}_t adapted processes, i.e., adjoint process \mathbf{y}_t and control process $\{\mathbf{z}_t^i\}_{i=1}^l$, should be found so as to simultaneously comply with the backward SDE and follow the terminal condition in (4). There are numerous mechanisms to find such processes, including mesh-based approaches and parameterization methods (Chessari et al., 2023; Yong & Jiang, 2023). The former considers pre-determined grid meshes for the process \mathbf{x}_t , and then obtains the processes $(\mathbf{y}_t, \{\mathbf{z}_t^i\}_{i=1}^l)$ as a function of considered meshes. However, this methodology needs extensive computations and suffers from the curse of dimensionality (Archibald

et al., 2020). In the parameterization methods, the processes $(\mathbf{y}_t, \{\mathbf{z}_t^i\}_{i=1}^l)$ are parameterized, e.g. using a neural network, such that the adjoint equation Equation (4) is fulfilled (Chessari et al., 2023). For our simulations, we leverage the parameterization methodology, and we term it as **Adjoint Gradient Projection** (Ad-GPro). With *ideal* parameterization, this method obtains the exact solution Ji et al. (2022); Chessari et al. (2023) and thus provides a benchmark for the comparison.

6.2 Stochastic Gradient Descent Method

This algorithm, which provides an computationally efficient approach, has been built on stochastic procedure based on Equation (5). In contrast to Ad-GPro, it approximates the process $(\mathbf{y}_t, \{\mathbf{z}_t^i\}_{i=1}^l)$ using a single-sample approximation and through a backward simulation mechanism (Archibald et al., 2020; Wang & Liu, 2025). This methodology thus reduces the extensive computations of Ad-GPro at the cost of performance decrease or requiring more update iterations for convergence. We term this algorithm as **Adjoint Stochastic Gradient Descent** (Ad-SGD).

7 Experiments

We here consider scalar and vector experiments of stochastic optimal control problems for the evaluation purposes. We then benchmark our proposed algorithm Mal-GPro against Adjoint sensitivity based algorithms, i.e., Ad-SGD and Ad-GPro.

7.1 Scalar SOCPs

Algorithms Setup: For all of the considered algorithms, we set the number of batches to 100, and learning rate to $\lambda = 10^{-2}$, unless specified. For the Ad-GPro, we use a neural network parameterization to estimate the adjoint/control processes $(\mathbf{y}_t, \{\mathbf{z}_t^i\}_{i=1}^l)$. For this, we apply 3 hidden layers with 16 neurons and *tanh* activation function.

Experiment 1: We now consider a Black-Scholes type control problem Du & Shi (2013)

$$\begin{aligned} \min_{u \in \mathcal{U}} J(u, x_0) &= \frac{1}{2} \int_0^T \mathbb{E}[(x_t - x_t^*)^2] dt + \frac{1}{2} \int_0^T u_t^2 dt, \\ \text{s.t. } dx_t &= u_t x_t dt + \sigma x_t dw_t, \end{aligned} \quad (22)$$

with $x_0 = 1$, $T = 1$, $x_t^* = \frac{e^{\sigma^2 t} - (T - t)^2}{1/x_0 - Tt + \frac{t^2}{2}} + 1$, and $\sigma = 0.01$ as the diffusion coefficient. The following analytical solution then can be found as a benchmark: $u_t^a = \frac{T-t}{1/x_0 - Tt + \frac{t^2}{2}}$,

Figure 1 shows the results of our Mal-GPro algorithm compared to the baseline algorithms, Ad-SGD and Ad-GPro, for this problem. Based on Figure 1a, all of the considered algorithms show the same behavior from the perspectives of performance and sample-efficiency (the update iterations it takes to converge). Moreover, all of the algorithms can properly learn the control decision and their respective solutions match with the analytical solution. We also evaluate the control error of different schemes defined as below.

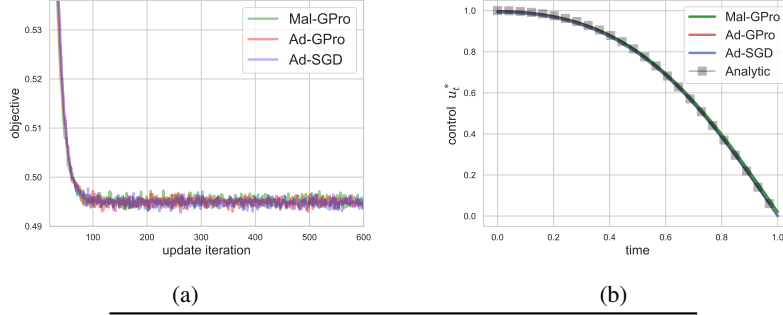
$$\mathcal{E}_c = \int_0^T \|\mathbf{u}_t^* - \mathbf{u}_t^a\|^2 dt, \quad (23)$$

where \mathbf{u}_t^* is the optimal control obtained by considered algorithms (Mal-GPro, Ad-GPro and Ad-SGD), and \mathbf{u}_t^a is the analytical control decision. Table 1c shows the control error \mathcal{E}_c of different schemes. Mal-GPro algorithm needs smaller step-size to reach an extent of control error comparable to Ad-SGD and Ad-GPro.

Experiment 2: We now consider the following optimal control problem Du & Shi (2013).

$$\begin{aligned} \min_{u \in \mathcal{U}} J(u, x_0) &= \frac{1}{2} \int_0^T \mathbb{E}[(x_t - 1)^2] dt + \frac{1}{2} \int_0^T u_t^2 dt, \\ \text{s.t. } dx_t &= u_t x_t dt + \sigma \sqrt{1 + x_t^2} dw_t, \end{aligned} \quad (24)$$

with given $x_0 = 1$, $T = 1$ and $\sigma = 0.5$ as the diffusion coefficient. However, the analytical solution of this problem is not known.



Model	Control Error \mathcal{E}_c
Ad-GPro, ($\Delta t = 10^{-2}$)	$2.2 \times 10^{-5} \pm 2 \times 10^{-8}$
Ad-SGD, ($\Delta t = 10^{-2}$)	$5.5 \times 10^{-5} \pm 7 \times 10^{-7}$
Mal-GPro, ($\Delta t = 10^{-2}$)	$8.9 \times 10^{-5} \pm 1 \times 10^{-7}$
Mal-GPro, ($\Delta t = 5 \times 10^{-3}$)	$1.7 \times 10^{-5} \pm 6 \times 10^{-8}$

(c)

Figure 1: The results of our Mal-GPro algorithm compared to the baseline algorithms, Ad-SGD and Ad-GPro, for problem (22). (a) shows the optimum value of objective, and (b) shows the optimum control decision. Clearly, all of the considered algorithm can properly learn the control decision and their respective solutions match with the analytical one. (c) tabulates the control error \mathcal{E}_c (integral of L2-norm of difference between the obtained control and the analytical one) of different schemes; Mal-GPro algorithm needs smaller step-size to reach a level of error comparable to Ad-SGD and Ad-GPro.

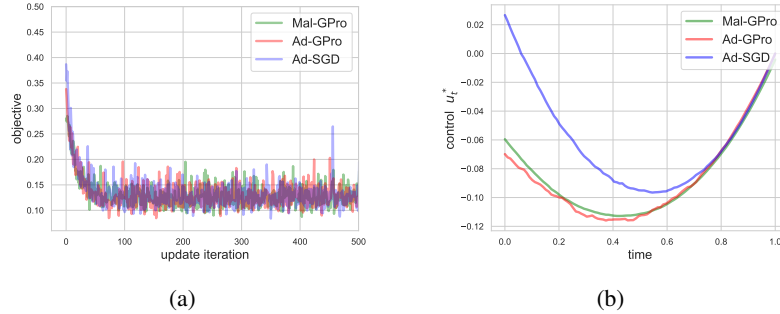
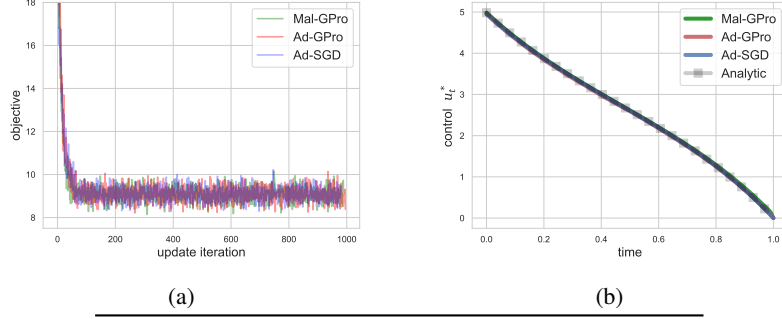


Figure 2: The results of our Mal-GPro algorithm compared to the baseline algorithms, Ad-SGD and Ad-GPro, for problem (24). (a) shows the optimum value of objective and (b) the optimum control decision. While Ad-SGD cannot provide a proper solution, the control trajectories of Mal-GPro and Ad-GPro approximately coincide. The control trajectory produced by Ad-GPro appears non-smooth due to the inherent limited capacity of the parametric approximation used in simulating the adjoint process.

Figure 2 shows the results of Mal-GPro algorithm compared to Ad-SGD and Ad-GPro algorithms, for this problem. According to Figure 2b, the control trajectories of Mal-GPro and Ad-GPro approximately coincide, while the solution of Ad-SGD deviates from them. The reason is that Ad-SGD provides an approximation mechanism and it is not guaranteed to obtain the optimal solution Archibald et al. (2020). Note that, the control trajectory produced by Ad-GPro appears non-smooth due to the inherent limited capacity of the parametric approximation used in simulating the adjoint process. These results portrays the effectiveness of Mal-GPro for solving SOCPs.

7.2 Vector SOCPs

Algorithms Setup: For all of the considered algorithms, we set the number of batches to 100, and the learning rate to $\lambda \in [10^{-2}, 3 \times 10^{-2}]$. For the Ad-GPro, we use a neural network parameterization



Model	Control Error \mathcal{E}_c
Ad-GPro, ($\Delta t = 10^{-2}$)	$8.2 \times 10^{-4} \pm 1.3 \times 10^{-4}$
Ad-SGD, ($\Delta t = 10^{-2}$)	$2.2 \times 10^{-4} \pm 1.5 \times 10^{-4}$
Mal-GPro, ($\Delta t = 10^{-2}$)	$6.5 \times 10^{-4} \pm 9 \times 10^{-5}$
Mal-GPro, ($\Delta t = 5 \times 10^{-3}$)	$2.5 \times 10^{-4} \pm 1 \times 10^{-4}$

(c)

Figure 3: The results of our Mal-GPro algorithm compared to the baseline algorithms, Ad-SGD and Ad-GPro, for problem (25). (a) shows the optimum value of objective and (b) the optimum control decision. Clearly, all of the considered algorithm can properly learn the control decision and their respective solutions match with the analytical one. (c) tabulates the control error \mathcal{E}_c of different schemes; Mal-GPro algorithm needs smaller step-size to reach a level of error comparable to Ad-SGD and Ad-GPro.

to estimate the adjoint/control processes $(\mathbf{y}_t, \{\mathbf{z}_t^i\}_{i=1}^l)$. For this, we apply 3 hidden layers with 16 neurons and *tanh* activation function.

Experiment 1: We consider the following SOCP with 3-dimensional controlled process Archibald et al. (2020)

$$\begin{aligned} \min_{u \in \mathcal{U}} J(u, \mathbf{x}_0) &= \frac{1}{2} \left[\int_0^T \mathbb{E} \left\{ (\mathbf{x}_t - \mathbf{x}_t^*)^\top \mathbf{C} (\mathbf{x}_t - \mathbf{x}_t^*) \right\} dt + \int_0^T u_t^2 dt \right], \\ \text{s.t. } d\mathbf{x}_t &= (u_t \mathbf{1} - \mathbf{r}_t) dt + \mathbf{I} d\mathbf{w}_t, \quad \mathbf{x}_t \in \mathbb{R}^3, \end{aligned} \quad (25)$$

with $\mathbf{x}_0 = -\mathbf{1}$, where $\mathbf{1} = (1, 1, 1)^\top$, $u_t \in \mathbb{R}$ is the control process, $\mathbf{r}_t = \frac{t}{2} \mathbf{1}$, $\mathbf{C} = \begin{pmatrix} 3 & 0 & 0 \\ 0 & 1 & 0 \\ 0 & 0 & 2 \end{pmatrix}$ and $\mathbf{x}_t^* = (3Tt - \frac{t^2}{2}) \mathbf{1} + (-\frac{1}{2}, 0, 1)^\top$. It has the following analytical solution for the control decision.

$$u_t^a = 3T - t/2 - \frac{2.5 \cosh(\sqrt{6}t) + \sqrt{6} \sinh(\sqrt{6}(t - T))}{\cosh(\sqrt{6}T)}$$

Figure 3 shows the results of our Mal-GPro algorithm compared to the baseline algorithms, Ad-SGD and Ad-GPro. Clearly, all of the considered algorithm have the same behavior from performance and sample-efficiency viewpoints, and can properly learn control decisions matching with the analytical solution. Figure 3c tabulates the *control error* of different schemes; Mal-GPro algorithm needs smaller step-size to reach a level of error comparable to Ad-SGD.

Experiment 2: We now consider the following vector problem Mohamed et al. (2022):

$$\begin{aligned} \min_{\mathbf{u} \in \mathcal{U}} J(\mathbf{u}, \mathbf{x}_0) &:= \mathbb{E} \left\{ \int_0^T (\mathbf{x}_t^\top \mathbf{R} \mathbf{x}_t + \mathbf{u}_t^\top \mathbf{C} \mathbf{u}_t) dt \right\} \\ \text{s.t. } d\mathbf{x}_t &= \mathbf{a}(\mathbf{x}_t, \mathbf{u}_t) dt + \mathbf{b}(\mathbf{x}_t, \mathbf{u}_t) d\mathbf{w}_t, \end{aligned} \quad (26)$$

where $\mathbf{x}_0 = -\mathbf{1}$, $T = 1$, $\mathbf{R} = \begin{pmatrix} 1 & 0 \\ 0 & 2 \end{pmatrix}$, $\mathbf{C} = \begin{pmatrix} 1 & 0 \\ 0 & 4 \end{pmatrix}$, $\mathbf{a}(\mathbf{x}_t, \mathbf{u}_t) = \begin{pmatrix} -x_{t,0} - 2x_{t,1}^2 - x_{t,2}^3/2 + u_{t,0} \\ -\cos(x_{t,1}) + u_{t,1} \end{pmatrix}$, $\mathbf{b}(\mathbf{x}_t, \mathbf{u}_t) = \begin{pmatrix} 0.4 + u_{t,0} \\ 0.2 + 2u_{t,1} \end{pmatrix}$ and $\mathcal{U} = \{\mathbf{u} \in \mathbb{R}^2 \mid -1 \leq u_i \leq 1, i \in \{0, 1\}\}$.

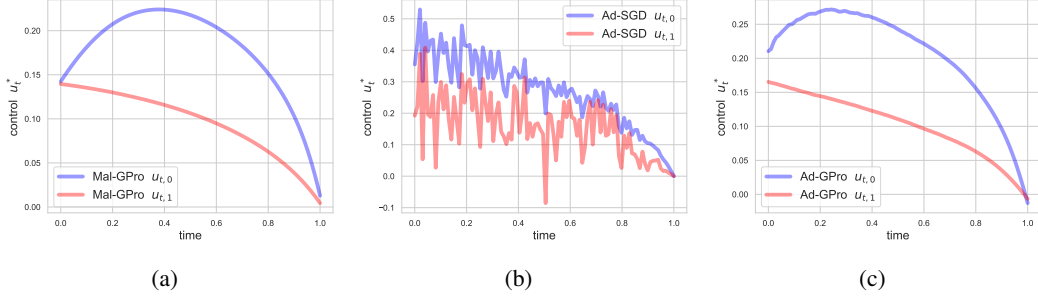


Figure 4: The performance of Mal-GPro algorithms on SOCP (26), compared to the baseline approaches Ad-GPro and Ad-SGD. (a) shows the control vector by Mal-GPro, (b) the control vector found by Ad-SGD, and (c) the control vector by Ad-GPro. In contrast to Mal-GPro, Ad-SGD cannot properly find the optimum control decision.

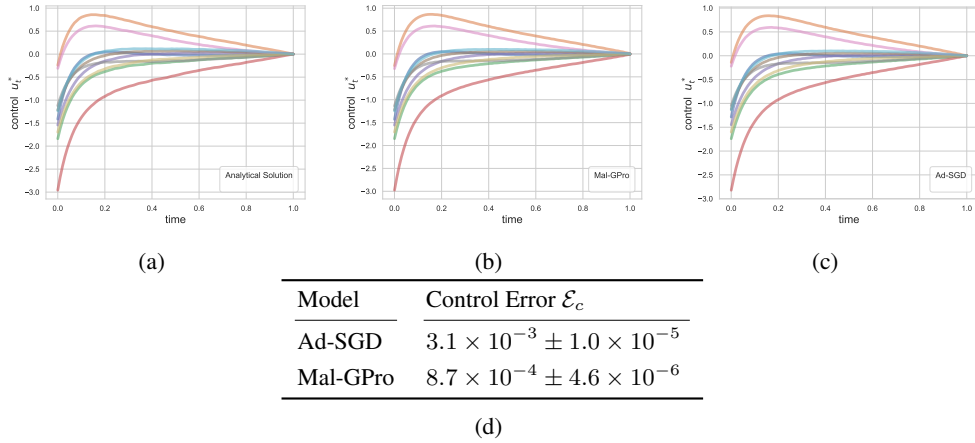


Figure 5: The results of our Mal-GPro algorithm compared to the baseline algorithm Ad-SGD for problem (27) with $\Delta t = 10^{-2}$. (a) shows the analytical control solution, and (b)-(c) show the control decisions obtained by Mal-GPro and Ad-SGD. Clearly, all of them find the same control solutions. (d) tabulates the control error \mathcal{E}_c of Mal-GPro against Ad-SGD. Our algorithm develops lower control error with less variance compared to Ad-SGD for this problem.

Figures 4a to 4c illustrate the obtained control decision for Ad-SGD, Mal-GPro and Ad-GPro, respectively, on SOCP (26). In contrast to Mal-GPro, Ad-SGD cannot properly find the optimum control decision. There is slight difference between control solutions of Mal-GPro and Ad-GPro due to the limited capacity of the parametric methodology in Ad-GPro. It again shows the effectiveness of Mal-GPro in obtaining optimal solution for SOCPs, compared to the baseline algorithms.

Experiment 3: We now consider a Linear-Quadratic (LQ) control problem as a high-dimensional SOCP benchmark (Pham, 2009; Sun & Yong, 2020):

$$\begin{aligned} \min_{\mathbf{u} \in \mathcal{U}} J(\mathbf{u}, \mathbf{x}_0) &:= \mathbb{E} \left\{ \frac{1}{2} \int_0^T (\mathbf{x}_t^\top \mathbf{Q} \mathbf{x}_t + \mathbf{u}_t^\top \mathbf{R} \mathbf{u}_t) dt \right\} \\ \text{s.t. } d\mathbf{x}_t &= (\mathbf{A} \mathbf{x}_t + \mathbf{B} \mathbf{u}_t) dt + \Sigma d\mathbf{w}_t, \end{aligned} \quad (27)$$

For this experiment, we set $n = k = 10$, $\mathbf{A} = -0.5\mathbf{U}_1$ and $\mathbf{B} = \mathbf{U}_2$, where $\{\mathbf{U}_i\}_{i=1}^2$ are matrices with elements uniformly selected within $[0, 1]$. Moreover, $\mathbf{Q} = \mathbf{I}$, $\mathbf{R} = 0.1\mathbf{I}$, and $\Sigma = \nu\mathbf{I}$ where $\nu = 0.3$ is the volatility coefficient (Domingo-Enrich et al., 2024). Note that this problem, known as linear quadratic regulator (LQR), have an analytical control solution that can be obtained based on the Riccati equation (Sun & Yong, 2020).

Although, we do not evaluate Ad-GPro due to its computational complexity, the analytical solution can be obtained as a benchmark for this problem. Figure 5 illustrates the analytical control decision

Table 1: Average runtime per iteration update (seconds) for our method Mal-GPro versus baselines Ad-GPro and Ad-SGD evaluated on SOCPs (25),(26) and (27) with $n = k = 5$.

Problem	Mal-GPro	Ad-SGD	Ad-GPro
SOCP (25)	0.5	0.1	12.0
SOCP (26)	0.3	0.1	11.0
SOCP (27)	0.8	0.1	26.6

Note: Reported values are per-iteration averages computed over independent runs (mean over iterations). Measurements were taken on CPU Core i5-13600H with 32 GB RAM.

and learned decisions of Mal-GPro algorithm and baseline Ad-SGD on SOCP (27). Clearly, all of them find the same control decision. However, Figure 5d tabulates the control error \mathcal{E}_c of Mal-GPro against Ad-SGD. Our algorithm develops lower error and with less variance compared to the Ad-SGD for this problem.

Average runtime: We now benchmark different algorithms from average runtime perspective, i.e., the average time required for methods run one iteration update. For this, we consider experiments in Equations (25) to (27). Table 1 compares our algorithm Mal-GPro against baseline methods Ad-GPro and Ad-SGD in terms of average runtime metric. Mal-GPro and Ad-SGD are time-efficient while Ad-GPro is considerably more time-consuming. Ad-SGD has been able to perform with least runtime by sacrificing the precision as the results in Figures 2b and 4b illustrate.

These results altogether show the effectiveness of Mal-GPro compared to baseline methods. Specifically, it highlights its efficiency against Ad-SGD from the performance viewpoint as well as against Ad-GPro from the computational complexity perspective.

8 Conclusion

In this paper, we leveraged Malliavin calculus to derive a stochastic maximum principle for stochastic optimal control problems (SOCPs). Accordingly, we derived a gradient projection algorithm to sequentially solve some classes of SOCPs. The experimental results show that our algorithm, at the same time can provide competitive performance against the standard iterative algorithms, and does not suffer from the dimensionality challenge of the standard approaches. The reason is that our algorithm replaces the need of backward SDEs with a Malliavin derivative that hopefully can be computed accurately based on a forward simulator.

References

- Alòs, E. and García Lorite, D. *Malliavin Calculus in Finance: Theory and Practice*. Chapman and Hall/CRC Financial Mathematics Series. Chapman and Hall/CRC, Boca Raton, FL, 2021. ISBN 9780367893446.
- Archibald, R., Bao, F., and Yong, J. A stochastic gradient descent approach for stochastic optimal control. *East Asian Journal on Applied Mathematics*, 10(4):635–658, 2020. doi: 10.4208/eajam.190420.200420. URL <https://doi.org/10.4208/eajam.190420.200420>.
- Bouchard, B., Elie, R., and Moreau, L. Regularity of BSDEs with a convex constraint on the gains-process. *Bernoulli*, 24(3):1613–1635, 2018.
- Chessari, J., Kawai, R., Shinozaki, Y., and Yamada, T. Numerical methods for backward stochastic differential equations: A survey. *Probability Surveys*, 20:486–567, 2023. doi: 10.1214/23-PS18.
- Domingo-Enrich, C., Han, J., Amos, B., Bruna, J., and Chen, R. T. Q. Stochastic optimal control matching. In *The Thirty-eighth Annual Conference on Neural Information Processing Systems*, 2024. URL <https://openreview.net/forum?id=wFU2CdgmWt>.
- Du, N. and Shi, J. An effective gradient projection method for stochastic optimal control. *International Journal of Numerical Analysis and Modeling*, 10(4):757–774, 2013.

- Geng, J., Hu, Y., Niu, J., and Tang, S. A maximum principle for stochastic optimal control with terminal state constraints, and its applications. *Journal of Mathematical Analysis and Applications*, 500(2):125139, 2021. doi: 10.1016/j.jmaa.2021.125139.
- Gobet, E. and Munos, R. Sensitivity analysis using itô–malliavin calculus and martingales, and application to stochastic optimal control. *SIAM Journal on Control and Optimization*, 43(5): 1676–1713, 2005. doi: 10.1137/S0363012902419059.
- Gong, B., Liu, W., Tang, T., Zhao, W., and Zhou, T. An efficient gradient projection method for stochastic optimal control problems. *SIAM Journal on Numerical Analysis*, 55(6):2982–3005, 2017. doi: 10.1137/17M1123559.
- Hientzsch, B. Introduction to solving quant finance problems with time-stepped FBSDE and deep learning. *arXiv preprint arXiv:1911.12231*, 2019.
- Ji, S., Peng, S., Peng, Y., and Zhang, X. Solving stochastic optimal control problem via stochastic maximum principle with deep learning method. *Journal of Scientific Computing*, 93(1), October 2022. ISSN 0885-7474. doi: 10.1007/s10915-022-01979-5. URL <https://doi.org/10.1007/s10915-022-01979-5>.
- Kloeden, P. E. and Platen, E. *Numerical Solution of Stochastic Differential Equations*, volume 23 of *Applications of Mathematics*. Springer-Verlag, Berlin, Heidelberg, 1992. ISBN 978-3-662-12616-5. doi: 10.1007/978-3-662-12616-5.
- Ma, J. and Yong, J. *Forward-Backward Stochastic Differential Equations and their Applications*, volume 1702 of *Lecture Notes in Mathematics*. Springer, 1999.
- Meyer-Brandis, T., Øksendal, B., and Zhou, X. A mean-field stochastic maximum principle via malliavin calculus. *Stochastics*, 84(5-6):643–666, 2012. doi: 10.1080/17442508.2011.647717.
- Mohamed, M. N. G., Chakravorty, S., Goyal, R., and Wang, R. On the feedback law in stochastic optimal nonlinear control. In *2022 American Control Conference (ACC)*, pp. 970–975, 2022. doi: 10.23919/ACC53348.2022.9867673.
- Nualart, D. and Nualart, E. *Introduction to Malliavin Calculus*. Cambridge University Press, Cambridge, 2018. ISBN 9781107611986.
- Pham, H. *Continuous-Time Stochastic Control and Optimization with Financial Applications*, volume 61 of *Stochastic Modelling and Applied Probability*. Springer, Berlin, Heidelberg, 2009. ISBN 978-3-540-89499-5. doi: 10.1007/978-3-540-89500-8.
- Sun, J. and Yong, J. *Stochastic Linear-Quadratic Optimal Control Theory: Open-Loop and Closed-Loop Solutions*. SpringerBriefs in Mathematics. Springer, Cham, 1st edition, 2020. ISBN 978-3-030-20921-6.
- Wang, Q. and Liu, W. An efficient gradient projection method for stochastic optimal control problem with expected integral state constraint. *Journal of Scientific Computing*, 102(3):71, 2025. doi: 10.1007/s10915-024-02777-x. URL <https://doi.org/10.1007/s10915-024-02777-x>. Published January 27, 2025.
- Yong, J. and Jiang, Y. Forward-backward stochastic differential equations: Initiation, development and beyond. *Numerical Algebra, Control and Optimization*, 13(3&4):367–391, jan 2023. doi: 10.3934/naco.2022011.
- Yong, J. and Zhou, X. Y. *Stochastic Controls: Hamiltonian Systems and HJB Equations*, volume 43 of *Stochastic Modelling and Applied Probability*. Springer, 1999.
- Zhang, J. *Backward Stochastic Differential Equations: From Linear to Fully Nonlinear Theory*, volume 86 of *Probability Theory and Stochastic Modelling*. Springer, 2017.
- Zhang, L. A BSDE approach to stochastic differential games involving impulse controls and HJBI equation. *Journal of Systems Science and Complexity*, 35(3):766–801, 2022.

A Proof of Theorem 4.1

To prove Theorem 4.1, we need the following Lemma:

Lemma A.1. Consider the diffusion process $X = (x_t)_{t \in [0, T]}$ following the SDE (7) with $n = k = 1$, i.e.,

$$dx_t = a(x_t, u_t)dt + b(x_t, u_t)dw_t.$$

The solution of the variational SDE

$$d\delta_t = (a_x(x_t, u_t)\delta_t + a_u(x_t, u_t)v_t)dt + (b_x(x_t, u_t)\delta_t + b_u(x_t, u_t)v_t)dw_t. \quad (28)$$

with $\delta_0 = 0$ is then expressed by

$$\delta_t = \int_0^t \frac{D_s x_t}{b(x_s, u_s)} (a_u(x_s, u_s) - b_x(x_s, u_s) b_u(x_s, u_s)) v_s ds + \int_0^t \frac{D_s x_t}{b(x_s, u_s)} b_u(x_s, u_s) v_s dw_s.$$

Proof. We first consider a SDE with the form of

$$d\eta_t = a_x(x_t, u_t)\eta_t dt + b_x(x_t, u_t)\eta_t dw_t. \quad (29)$$

By considering the variable transformation $e_t = \log(\eta_t)$ and applying Ito's formula, we can simply obtain the solution of η_t as

$$\eta_t = \exp \left(\int_0^t (a_x(x_t, u_t) - \frac{1}{2}b_x(x_t, u_t)^2)dt + \int_0^t b_x(x_t, u_t)dw_t \right) > 0. \quad (30)$$

Based on the variation-of-constant approach, the solution of δ_t can be obtained using

$$\delta_t = \eta_t q_t, \quad (31)$$

where q_t should be found. For $b_u = 0$, Ito's formula and some mathematical manipulations show that $dq_t = \eta_t^{-1}(a_u(x_t, u_t)v_t dt + b_u(x_t, u_t)v_t dw_t)$. However, for $b_u \neq 0$, we should set:

$$\eta_t dq_t = (a_u(x_t, u_t)v_t + \gamma_t) dt + (b_u(x_t, u_t)v_t + \mu_t) dw_t, \quad (32)$$

where γ_t and μ_t should be determined so that the dt-terms match after including the quadratic covariation. To obtain them, Equation (31) gives:

$$d\delta_t = d\eta_t q_t + \eta_t dq_t + d\eta_t dq_t,$$

which accordingly gives the following from Equations (28), (29) and (32):

$$\begin{aligned} & (\cancel{a_x(x_t, u_t)\delta_t} + \cancel{a_u(x_t, u_t)v_t})dt + (\cancel{b_x(x_t, u_t)\delta_t} + \cancel{b_u(x_t, u_t)v_t})dw_t \\ &= (a_x(x_t, u_t)\eta_t dt + b_x(x_t, u_t)\eta_t dw_t)q_t + (a_u(x_t, u_t)v_t + \gamma_t) dt + (b_u(x_t, u_t)v_t + \mu_t) dw_t \\ & \quad + b_x(x_t, u_t)\eta_t dw_t \eta_t^{-1}(b_u(x_t, u_t)v_t + \mu_t)dw_t \\ &= (\cancel{a_x(x_t, u_t)\delta_t} dt + \cancel{b_x(x_t, u_t)\delta_t} dw_t) + (\cancel{a_u(x_t, u_t)v_t} + \gamma_t) dt + (\cancel{b_u(x_t, u_t)v_t} + \mu_t) dw_t \\ & \quad + b_x(x_t, u_t)(b_u(x_t, u_t)v_t + \mu_t)dt. \end{aligned}$$

By canceling the similar terms, we then obtain:

$$\gamma_t = -b_x(x_t, u_t)b_u(x_t, u_t)v_t, \quad \mu_t = 0.$$

Considering that $q_0 = \eta_0^{-1}\delta_0 = 0$, we finally get:

$$\delta_t = \eta_t q_t = \int_0^t \eta_t \eta_s^{-1} (a_u(x_s, u_s) - b_x(x_s, u_s) b_u(x_s, u_s)) v_s ds + \int_0^t \eta_t \eta_s^{-1} b_u(x_s, u_s) v_s dw_s. \quad (33)$$

Now, based on Equation (30), one can get:

$$\eta_t \eta_s^{-1} = \exp \left(\int_s^t (a_x(x_t, u_t) - \frac{1}{2}b_x(x_t, u_t)^2)dt + \int_s^t b_x(x_t, u_t)dw_t \right),$$

which gives $\eta_t \eta_s^{-1} = \frac{D_s x_t}{b(x_s, u_s)}$ based on Equation (11). By substituting this into Equation (33), the statement thus follows. \square

We now present Theorem 4.1 with a proof. Note that without loss of generalization, we assume that $h(x_T) = 0$.

Theorem A.2. Consider SOCP P_1 (3) with $n = k = 1$, the variation of cost functional $J(u, x_0)$ along direction v , through Definition (3.1), can be obtained by:

$$\begin{aligned} \delta_v J(u, x_0) = & \int_0^T \mathbb{E} \left\{ \int_s^T \left(\frac{a_u(s) - b_x(s)b_u(s)}{b(s)} L_x(t) D_s x_t \right. \right. \\ & \left. \left. + \frac{b_u(s)}{b(s)} (L_{xx}(t) D_s x_t + L_{xu}(t) D_s u_t) D_s x_t \right) dt + L_u(s) \right\} v_s ds, \end{aligned}$$

where $D_s x_t$ is the Malliavin derivative of x_t against w_s , $L_x(t)$, $a_u(s)$, and $b(s)$ are short notations for $L_x(x_t, u_t, t)$, $a_u(x_s, u_s)$ and $b(x_s, u_s)$, respectively, with L_x and L_{xx} denoting the first and second gradients of L w.r.t x , and L_u , a_u , b_u showing the gradient of L , a and b w.r.t. u .

Proof. We perturb the control process u_t through $u_t + \epsilon v_t$, which leads to the diffusion process $x_t^{u_t + \epsilon v_t}$. We then define a variational process:

$$\delta_t^x := \lim_{\epsilon \rightarrow 0} \frac{1}{\epsilon} (x_t^{u_t + \epsilon v} - x_t^u).$$

Based on Equation (7), δ_t^x obeys the following variational SDE:

$$d\delta_t^x = (a_x(x_t, u_t) \delta_t^x + a_u(x_t, u_t) v_t) dt + (b_x(x_t, u_t) \delta_t^x + b_u(x_t, u_t) v_t) dw_t. \quad (34)$$

Using Lemma (A.1), the solution of this variational SDE is:

$$\delta_t^x = \int_0^t \frac{D_s x_t}{b(x_s, u_s)} (a_u(x_s, u_s) - b_x(x_s, u_s) b_u(x_s, u_s)) v_s ds + \int_0^t \frac{D_s x_t}{b(x_s, u_s)} b_u(x_s, u_s) v_s dw_s. \quad (35)$$

On the other hand, the variation of cost functional $J(u, x_0)$ along direction v obeys:

$$\delta_v J(u, x_0) = \mathbb{E} \left\{ \int_0^T (L_x(x_t, u_t, t) \delta_t^x + L_u(x_t, u_t, t) v_t) dt \right\}. \quad (36)$$

By plugging Equation (35) into Equation (36), we then have:

$$\begin{aligned} \delta_v J(u, x_0) = & \mathbb{E} \int_0^T L_x(x_t, u_t, t) \int_0^t \frac{D_s x_t}{b(x_s, u_s)} (a_u(x_s, u_s) - b_x(x_s, u_s) b_u(x_s, u_s)) v_s ds dt \\ & + \mathbb{E} \int_0^T L_x(x_t, u_t, t) \int_0^t \frac{D_s x_t}{b(x_s, u_s)} b_u(x_s, u_s) v_s dw_s dt + \mathbb{E} \int_0^T L_u(x_t, u_t, t) v_t dt. \end{aligned}$$

We then leverage the integration-by-parts (6) for the second term in RHS of recent equation:

$$\begin{aligned} \delta_v J(u, x_0) = & \mathbb{E} \int_0^T \int_0^t L_x(x_t, u_t, t) \frac{D_s x_t}{b(x_s, u_s)} (a_u(x_s, u_s) - b_x(x_s, u_s) b_u(x_s, u_s)) v_s ds dt \\ & + \mathbb{E} \int_0^T \int_0^t D_s L_x(x_t, u_t, t) \frac{D_s x_t}{b(x_s, u_s)} b_u(x_s, u_s) v_s ds dt + \mathbb{E} \int_0^T L_u(x_t, u_t, t) v_t dt. \end{aligned}$$

Changing the order of integrals then gives:

$$\begin{aligned} \delta_v J(u, x_0) = & \mathbb{E} \int_0^T \int_s^T L_x(x_t, u_t, t) \frac{D_s x_t}{b(x_s, u_s)} (a_u(x_s, u_s) - b_x(x_s, u_s) b_u(x_s, u_s)) dt v_s ds \\ & + \mathbb{E} \int_0^T \int_s^T D_s L_x(x_t, u_t, t) \frac{D_s x_t}{b(x_s, u_s)} b_u(x_s, u_s) dt v_s ds + \mathbb{E} \int_0^T L_u(x_t, u_t, t) v_t dt. \end{aligned}$$

where we used the chain rule $D_s L_x(x_t, u_t, t) = L_{xx}(x_t, u_t, t) D_s x_t + L_{xu}(x_t, u_t, t) D_s u_t$. Therefore, the statement proves. \square

B Proof of Theorem 4.3

To prove Theorem 4.3, we need some founding Lemmas. Before that we need to first recall the Stein's lemma that for zero-mean jointly Gaussian random variables $\mathbf{x} \in \mathbb{R}^n$ and $\mathbf{y} \in \mathbb{R}^n$, and a vector-valued continuously differentiable function $F : \mathbb{R}^n \rightarrow \mathbb{R}^n$, we can get:

$$\mathbb{E} \{ F(\mathbf{x})^\top \mathbf{y} \} = \text{tr} \{ \mathbb{E} \{ \mathcal{J}_x F(\mathbf{x}) \} \mathbb{E} \{ \mathbf{y} \mathbf{y}^\top \} \} \quad (37)$$

Lemma B.1. *Suppose $F : \mathbb{R}^n \rightarrow \mathbb{R}^n$ be a vector-valued random function in the domain of Malliavin derivative, $X = (\mathbf{x}_t)_t$ be a Wiener-driven and Malliavin differentiable process, and $\{\mathbf{G}^l = (\mathbf{g}_t^l)_t\}_{l=1}^d$ with $\mathbf{g}_t^l \in \mathbb{R}^n$ be an adapted and square-integrable process, we then get:*

$$\mathbb{E} \left\{ F(\mathbf{x}_t)^\top \sum_{l=1}^d \int_0^t \mathbf{g}_s^l dw_s^l \right\} = \sum_{l=1}^d \int_0^t \mathbb{E} \{ D_s^l F(\mathbf{x})^\top \mathbf{g}_s^l \} ds = \sum_{l=1}^d \int_0^t \mathbb{E} \{ D_s^l \mathbf{x}_t^\top \mathcal{J}_x F(\mathbf{x})^\top \mathbf{g}_s^l \} ds,$$

where $D_s^l \mathbf{x}_t$ is the Malliavin derivative of \mathbf{x}_t against the Wiener process w_t^l .

Proof. This theorem is the multivariate extension of integration-by-parts formula (see Section 3.2) in the Malliavin calculus. Without loss of generality, we provide a proof for the case of $\mathbf{x}_t = \int_0^t \sum_{l=1}^d \mathbf{h}_s^l dw_s^l$. The proof can be then generalized for the other cases (Nualart & Nualart, 2018; Alòs & García Lorite, 2021). Let $\mathcal{F}^{\mathbf{h}, \mathbf{g}}$ be the σ -algebra of processes \mathbf{h}^l and \mathbf{g}^l that encodes all the information of these process up to time t . We then get:

$$\begin{aligned} \mathbb{E} \left\{ F(\mathbf{x}_t)^\top \sum_{l=1}^d \int_0^t \mathbf{g}_s^l dw_s^l \right\} &= \mathbb{E}_{\mathcal{F}^{\mathbf{h}, \mathbf{g}}} \left\{ F(\mathbf{x}_t)^\top \sum_{l=1}^d \int_0^t \mathbf{g}_s^l dw_s^l \mid \mathcal{F}^{\mathbf{h}, \mathbf{g}} \right\} \\ &\stackrel{(a)}{=} \mathbb{E}_{\mathcal{F}^{\mathbf{h}, \mathbf{g}}} \text{tr} \left\{ \sum_{l=1}^d \mathbb{E} \left\{ \mathcal{J}_x F \mid \mathcal{F}^{\mathbf{h}, \mathbf{g}} \right\} \mathbb{E} \left\{ \int_0^t \mathbf{h}_s^l \mathbf{g}_s^{l \top} ds \mid \mathcal{F}^{\mathbf{h}, \mathbf{g}} \right\} \right\} \\ &= \mathbb{E}_{\mathcal{F}^{\mathbf{h}, \mathbf{g}}} \text{tr} \left\{ \sum_{l=1}^d \mathbb{E} \left\{ \mathcal{J}_x F \mid \mathcal{F}^{\mathbf{h}, \mathbf{g}} \right\} \int_0^t \mathbf{h}_s^l \mathbf{g}_s^{l \top} ds \right\} \\ &= \mathbb{E}_{\mathcal{F}^{\mathbf{h}, \mathbf{g}}} \text{tr} \left\{ \sum_{l=1}^d \mathbb{E} \left\{ \mathcal{J}_x F \int_0^t \mathbf{h}_s^l \mathbf{g}_s^{l \top} ds \mid \mathcal{F}^{\mathbf{h}, \mathbf{g}} \right\} \right\} \\ &\stackrel{(b)}{=} \mathbb{E}_{\mathcal{F}^{\mathbf{h}, \mathbf{g}}} \sum_{l=1}^d \int_0^t \mathbb{E} \left\{ \mathbf{g}_s^{l \top} \mathcal{J}_x F D_s^l \mathbf{x}_t \mid \mathcal{F}^{\mathbf{h}, \mathbf{g}} \right\} ds = \sum_{l=1}^d \int_0^t \mathbb{E} \left\{ \mathbf{g}_s^{l \top} \mathcal{J}_x F D_s^l \mathbf{x}_t \right\} ds \end{aligned}$$

where (a) obtained based on the Stein's lemma (37), and we used $\text{tr}\{\mathbf{A}\mathbf{z}\mathbf{z}^\top\} = \text{tr}\{\mathbf{z}^\top \mathbf{A}\mathbf{z}\}$ for (b) with vector \mathbf{z} and matrix \mathbf{A} . \square

Lemma B.2. *Consider the diffusion process $\mathbf{X} = (\mathbf{x}_t)_{t \in [0, T]}$ following the SDE (7), i.e.,*

$$d\mathbf{x}_t = \mathbf{a}(\mathbf{x}_t, \mathbf{u}_t)dt + \sum_{l=1}^d \mathbf{b}_l(\mathbf{x}_t, \mathbf{u}_t)dw_t^l.$$

The solution of the variational SDE

$$d\delta_t = (\mathcal{J}_x \mathbf{a}(\mathbf{x}_t, \mathbf{u}_t)\delta_t + \mathcal{J}_u \mathbf{a}(\mathbf{x}_t, \mathbf{u}_t)\mathbf{v}_t)dt + \sum_{l=1}^d (\mathcal{J}_x \mathbf{b}_l(\mathbf{x}_t, \mathbf{u}_t)\delta_t + \mathcal{J}_u \mathbf{b}_l(\mathbf{x}_t, \mathbf{u}_t)\mathbf{v}_t)dw_t^l. \quad (38)$$

with $\delta_0 = \mathbf{0}$, is then expressed by

$$\delta_t = \int_0^t \Gamma_{s,t} \left(\mathcal{J}_u \mathbf{a}(\mathbf{x}_s, \mathbf{u}_s) - \sum_{l, l'} q_{l, l'} \mathcal{J}_x \mathbf{b}_l(\mathbf{x}_s, \mathbf{u}_s) \mathcal{J}_u \mathbf{b}_{l'}(\mathbf{x}_s, \mathbf{u}_s) \right) \mathbf{v}_s ds + \int_0^t \sum_{l=1}^d \Gamma_{s,t} \mathcal{J}_u \mathbf{b}_l(\mathbf{x}_s, \mathbf{u}_s) \mathbf{v}_s dw_s^l,$$

where $q_{l, l'}$ is the diffusion coefficient between w_t^l and $w_t^{l'}$, and $\Gamma_{s,t} = \mathbf{Y}_t \mathbf{Z}_s$ follows the stochastic flows based on Equation (10).

Proof. For the ease of notations, we hereafter denote the arguments of functions, i.e. $(\mathbf{x}_t, \mathbf{u}_t)$ by merely (t) . We then consider a matrix SDE with the form of

$$d\Phi_t = \mathcal{J}_x \mathbf{a}(t) \Phi_t dt + \sum_{l=1}^d \mathcal{J}_x \mathbf{b}_l(t) \Phi_t dw_t^l, \quad \Phi_0 = \mathbf{I}, \quad (39)$$

where $\Phi_t \in \mathbb{R}^{n \times n}$ is assumed to be invertible. Notice that the solution for Φ_t that meets all of these conditions is the stochastic flow \mathbf{Y}_t (10). Based on the variation-of-constant approach, the solution of δ_t in (38) can be obtained using

$$\delta_t = \Phi_t \mathbf{q}_t, \quad (40)$$

where vector $\mathbf{q}_t \in \mathbb{R}^n$ should be found. For $\mathcal{J}_u \mathbf{b}_l = 0$, one can simply show that $\Phi_t d\mathbf{q}_t = \mathcal{J}_u \mathbf{a}(t) \mathbf{v}_t dt + \sum_{l=1}^d \mathcal{J}_u \mathbf{b}_l(t) \mathbf{v}_t dw_t^l$. However, in the case of $\mathcal{J}_u \mathbf{b}_l \neq 0$, we should set the following based on the Lemma (A.1):

$$\Phi_t d\mathbf{q}_t = (\mathcal{J}_u \mathbf{a}(t) \mathbf{v}_t + \Psi_t) dt + \sum_{l=1}^d \mathcal{J}_u \mathbf{b}_l(t) \mathbf{v}_t dw_t^l, \quad (41)$$

where $\Psi_t \in \mathbb{R}^{n \times n}$ now should be determined so that the dt-terms match after including the quadratic covariation. To obtain it, we take differential of Equation (40):

$$d\delta_t = d\Phi_t \mathbf{q}_t + \Phi_t d\mathbf{q}_t + d\Phi_t d\mathbf{q}_t,$$

which accordingly gives the following based on the Equations (38), (39) and (41):

$$\begin{aligned} & (\mathcal{J}_x \mathbf{a}(t) \delta_t + \mathcal{J}_u \mathbf{a}(t) \mathbf{v}_t) dt + \sum_{l=1}^d (\mathcal{J}_x \mathbf{b}_l(t) \delta_t dw_t^l + \mathcal{J}_u \mathbf{b}_l(t) \mathbf{v}_t dw_t^l) \\ &= \underbrace{\left(\mathcal{J}_x \mathbf{a}(t) \Phi_t dt + \sum_{l=1}^d \mathcal{J}_x \mathbf{b}_l(t) \Phi_t dw_t^l \right) \mathbf{q}_t}_{d\Phi_t \mathbf{q}_t} + \underbrace{(\mathcal{J}_u \mathbf{a}(t) \mathbf{v}_t + \Psi_t) dt + \sum_{l=1}^d \mathcal{J}_u \mathbf{b}_l(t) \mathbf{v}_t dw_t^l}_{\Phi_t d\mathbf{q}_t} \\ &+ \underbrace{\sum_{l=1}^d \sum_{l'=1}^d \mathcal{J}_x \mathbf{b}_l(t) \Phi_t \Phi_t^{-1} \mathcal{J}_u \mathbf{b}_{l'}(t) \mathbf{v}_t dw_t^l dw_t^{l'}}_{d\Phi_t d\mathbf{q}_t} \\ &\stackrel{(a)}{=} \left(\mathcal{J}_x \mathbf{a}(t) \delta_t dt + \sum_{l=1}^d \mathcal{J}_x \mathbf{b}_l(t) \delta_t dw_t^l \right) + (\mathcal{J}_u \mathbf{a}(t) \mathbf{v}_t + \Psi_t) dt + \sum_{l=1}^d \mathcal{J}_u \mathbf{b}_l(t) \mathbf{v}_t dw_t^l \\ &+ \sum_{l=1}^d \sum_{l'=1}^d \mathcal{J}_x \mathbf{b}_l(t) \mathcal{J}_u \mathbf{b}_{l'}(t) \mathbf{v}_t q_{l,l'} dt, \end{aligned}$$

where for (a), we used $dw_t^l dw_t^{l'} = q_{l,l'} dt$ and $\delta_t = \Phi_t \mathbf{q}_t$ based on Equation (40). By canceling the similar terms, we then obtain:

$$\Psi_t = - \sum_{l,l'}^d q_{l,l'} \mathcal{J}_x \mathbf{b}_l(t) \mathcal{J}_u \mathbf{b}_{l'}(t) \mathbf{v}_t.$$

Plugging the recent equation into Equation (41), utilization of Equation (40) and considering that $\mathbf{q}_0 = \mathbf{0}$ as $\delta_t = \mathbf{0}$ and Φ_0 is invertible, thus gives:

$$\delta_t = \Phi_t \mathbf{q}_t = \int_0^t \Phi_t \Phi_s^{-1} \left(\mathcal{J}_u \mathbf{a}(s) - \sum_{l,l'}^d q_{l,l'} \mathcal{J}_x \mathbf{b}_l(s) \mathcal{J}_u \mathbf{b}_{l'}(s) \right) \mathbf{v}_s ds + \int_0^t \sum_{l=1}^d \Phi_t \Phi_s^{-1} \mathcal{J}_u \mathbf{b}_l(s) \mathbf{v}_s dw_s^l. \quad (42)$$

As declared, Φ_t is equal to the stochastic flow \mathbf{Y}_t (10). Hence, based on Equation (9), we can get:

$$\Phi_t \Phi_s^{-1} = \Gamma_{s,t},$$

By substituting this into Equation (42), the statement thus follows. \square

We now present Theorem 4.3 with a proof. Note that without loss of generalization, we assume that $h(\mathbf{x}_T) = 0$.

Theorem B.3. Consider SOCP P_1 (3), the variation of cost functional $J(\mathbf{u}, \mathbf{x}_0)$ along direction \mathbf{v} , through Definition (3.1), can be obtained by:

$$\begin{aligned} \delta_{\mathbf{v}} J(\mathbf{u}, \mathbf{x}_0) = & \mathbb{E} \int_0^T \left\{ \left(\int_s^T \nabla_{\mathbf{x}} L(t)^\top \mathbf{\Gamma}_{s,t} dt + \nabla_{\mathbf{x}} h(\mathbf{x}_T)^\top \mathbf{\Gamma}_{s,T} \right) \left(\mathcal{J}_{\mathbf{u}} \mathbf{a}(s) - \sum_{l,l'}^d q_{l,l'} \mathcal{J}_{\mathbf{x}} \mathbf{b}_l(s) \mathcal{J}_{\mathbf{u}} \mathbf{b}_{l'}(s) \right) \right. \\ & + \sum_{l=1}^d \left(\int_s^T (D_s^l \mathbf{x}_t^\top \nabla_{\mathbf{x}}^2 L(t) + D_s^l \mathbf{u}_t^\top \nabla_{\mathbf{u}\mathbf{x}} L(t)) \mathbf{\Gamma}_{s,t} dt + D_s^l \mathbf{x}_T^\top \nabla_{\mathbf{x}}^2 h(\mathbf{x}_T) \mathbf{\Gamma}_{s,T} \right) \mathcal{J}_{\mathbf{u}} \mathbf{b}_l(s) \\ & \left. + \nabla_{\mathbf{u}} L(s)^\top \right\} \mathbf{v}_s ds, \end{aligned}$$

where $\mathbf{B} = [\mathbf{b}_1, \dots, \mathbf{b}_d]$, $\mathbf{\Gamma}_{s,t}$ relates to the Malliavin derivative $D_s \mathbf{x}_t$ through Equation (9), $q_{l,l'}$ is the diffusion coefficient between Wiener processes w_t^l and $w_t^{l'}$, $[\mathbf{A}]_l$ outputs the l -th column of matrix \mathbf{A} , and $\mathcal{J}_{\mathbf{x}} \mathbf{a}$ (respectively, $\mathcal{J}_{\mathbf{u}} \mathbf{a}$) stands for the Jacobian matrix of vector \mathbf{a} w.r.t. \mathbf{x} (respectively, \mathbf{u}).

Proof. We perturb the control decision \mathbf{u}_t through $\mathbf{u}_t + \epsilon \mathbf{v}_t$, which leads to the diffusion process $\mathbf{x}_t^{\mathbf{u}_t + \epsilon \mathbf{v}_t}$. We then define a variational process:

$$\delta_t^x := \lim_{\epsilon \rightarrow 0} \frac{1}{\epsilon} (\mathbf{x}_t^{\mathbf{u}_t + \epsilon \mathbf{v}_t} - \mathbf{x}_t^{\mathbf{u}}).$$

Based on Equation (7), δ_t^x obeys the following variational SDE:

$$d\delta_t^x = (\mathcal{J}_{\mathbf{x}} \mathbf{a}(t) \delta_t^x + \mathcal{J}_{\mathbf{u}} \mathbf{a}(t) \mathbf{v}_t) dt + \sum_{l=1}^d (\mathcal{J}_{\mathbf{x}} \mathbf{b}_l(t) \delta_t^x + \mathcal{J}_{\mathbf{u}} \mathbf{b}_l(t) \mathbf{v}_t) dw_t^l. \quad (43)$$

Using Lemma (B.2), the solution of this variational SDE is:

$$\delta_t^x = \int_0^t \mathbf{\Gamma}_{s,t} \left(\mathcal{J}_{\mathbf{u}} \mathbf{a}(s) - \sum_{l,l'}^d q_{l,l'} \mathcal{J}_{\mathbf{x}} \mathbf{b}_l(s) \mathcal{J}_{\mathbf{u}} \mathbf{b}_{l'}(s) \right) \mathbf{v}_s ds + \int_0^t \sum_{l=1}^d \mathbf{\Gamma}_{s,t} \mathcal{J}_{\mathbf{u}} \mathbf{b}_l(s) \mathbf{v}_s dw_s^l. \quad (44)$$

On the other hand, the variation of cost functional $J(\mathbf{u}, \mathbf{x}_0)$ along direction \mathbf{v} obeys:

$$\delta_{\mathbf{v}} J(\mathbf{u}, \mathbf{x}_0) = \mathbb{E} \left\{ \int_0^T (\nabla_{\mathbf{x}} L(t)^\top \delta_t^x + \nabla_{\mathbf{u}} L(t)^\top \mathbf{v}_t) dt \right\}. \quad (45)$$

By plugging Equation (44) into Equation (45), we then have:

$$\begin{aligned} \delta_{\mathbf{v}} J(\mathbf{u}, \mathbf{x}_0) = & \mathbb{E} \int_0^T \nabla_{\mathbf{x}} L(t)^\top \int_0^t \mathbf{\Gamma}_{s,t} \left(\mathcal{J}_{\mathbf{u}} \mathbf{a}(s) - \sum_{l,l'}^d q_{l,l'} \mathcal{J}_{\mathbf{x}} \mathbf{b}_l(s) \mathcal{J}_{\mathbf{u}} \mathbf{b}_{l'}(s) \right) \mathbf{v}_s ds dt \\ & + \mathbb{E} \int_0^T \sum_{l=1}^d \nabla_{\mathbf{x}} L(t)^\top \int_0^t \mathbf{\Gamma}_{s,t} \mathcal{J}_{\mathbf{u}} \mathbf{b}_l(s) \mathbf{v}_s dw_s^l dt + \mathbb{E} \int_0^T \mathcal{J}_{\mathbf{u}} L(t)^\top \mathbf{v}_t dt. \end{aligned}$$

We then apply the integration-by-parts Lemma (B.1) for the second term of RHS of the recent equation:

$$\begin{aligned} \delta_{\mathbf{v}} J(\mathbf{u}, \mathbf{x}_0) = & \mathbb{E} \int_0^T \int_0^t \nabla_{\mathbf{x}} L(t)^\top \mathbf{\Gamma}_{s,t} \left(\mathcal{J}_{\mathbf{u}} \mathbf{a}(s) - \sum_{l,l'}^d q_{l,l'} \mathcal{J}_{\mathbf{x}} \mathbf{b}_l(s) \mathcal{J}_{\mathbf{u}} \mathbf{b}_{l'}(s) \right) \mathbf{v}_s ds dt \\ & + \mathbb{E} \int_0^T \int_0^t \sum_{l=1}^d (D_s^l \mathbf{x}_t^\top \nabla_{\mathbf{x}}^2 L(t) + D_s^l \mathbf{u}_t^\top \nabla_{\mathbf{u}\mathbf{x}} L(t)) \mathbf{\Gamma}_{s,t} \mathcal{J}_{\mathbf{u}} \mathbf{b}_l(s) \mathbf{v}_s ds dt \\ & + \mathbb{E} \int_0^T \mathcal{J}_{\mathbf{u}} L(t)^\top \mathbf{v}_t dt, \end{aligned}$$

where $D_s^l \mathbf{x}_t$ (respectively, $D_s^l \mathbf{u}_t$) is the Malliavin derivative of \mathbf{x}_t (respectively, \mathbf{u}_t) against w_t^l . Changing the order of integrals then gives:

$$\begin{aligned} \delta_{\mathbf{v}} J(\mathbf{u}, \mathbf{x}_0) &= \mathbb{E} \int_0^T \int_s^T \nabla_{\mathbf{x}} L(t)^\top \Gamma_{s,t} \left(\mathcal{J}_{\mathbf{u}} \mathbf{a}(s) - \sum_{l,l'}^d q_{l,l'} \mathcal{J}_{\mathbf{x}} \mathbf{b}_l(s) \mathcal{J}_{\mathbf{u}} \mathbf{b}_{l'}(s) \right) dt \mathbf{v}_s ds \\ &+ \mathbb{E} \int_0^T \int_s^T \sum_{l=1}^d (D_s^l \mathbf{x}_t^\top \nabla_{\mathbf{x}}^2 L(t) + D_s^l \mathbf{u}_t^\top \nabla_{\mathbf{u}\mathbf{x}} L(t)) \Gamma_{s,t} \mathcal{J}_{\mathbf{u}} \mathbf{b}_l(s) dt \mathbf{v}_s ds \\ &+ \mathbb{E} \int_0^T \mathcal{J}_{\mathbf{u}} L(t)^\top \mathbf{v}_t dt. \end{aligned}$$

According to Equation (9), we have $D_s^l \mathbf{x}_t = [\Gamma_{s,t} \mathbf{B}(s)]_l$. This thus proves statement. \square

C proof of Proposition 5.3

According to Equation (8), the Malliavin derivative $D_r \mathbf{x}_t$ – for a given r and as a function of t – is a diffusion process adapted to the filtration \mathcal{F}_r . Therefore, based on Equation (9), the process $\Gamma_{r,t} := \mathbf{Y}_t \mathbf{Z}_r$, for a given r is adapted to \mathcal{F}_r . On the other hand, according to Equation (10) we can obtain

$$\begin{aligned} d\Gamma_{r,t} &= d\mathbf{Y}_t \mathbf{Z}_r = \mathcal{J}_{\mathbf{x}} \mathbf{a}(\mathbf{x}_t, \mathbf{u}_t) \mathbf{Y}_t \mathbf{Z}_r dt + \sum_{l=1}^d \mathcal{J}_{\mathbf{x}} \mathbf{b}_l(\mathbf{x}_t, \mathbf{u}_t) \mathbf{Y}_t \mathbf{Z}_r dw_t^l \\ &= \left(\sum_{l=1}^d \mathcal{J}_{\mathbf{x}} \mathbf{b}_l(\mathbf{x}_t, \mathbf{u}_t) dw_t^l + \mathcal{J}_{\mathbf{x}} \mathbf{a}(\mathbf{x}_t, \mathbf{u}_t) dt \right) \Gamma_{r,t}. \end{aligned}$$

Therefore, statement follows.